A rheological model for glassforming silicate melts in the systems CAS, MAS, MCAS

2007 J. Phys.: Condens. Matter 19 205148

(http://iopscience.iop.org/0953-8984/19/20/205148)

IOP PUBLISHING JOURNAL OF PHYSICS: CONDENSED MATTER

J. Phys.: Condens. Matter **19** (2007) 205148 (11pp) doi:10.1088/0953-8984/19/20/205148

A rheological model for glassforming silicate melts in the systems CAS, MAS, MCAS

Daniele Giordano[1,3] **and J K Russell**[2]

[1] Dipartimento di Scienze Geologiche, Università di Roma Tre, L.go S Leonardo Murialdo, 1, 00146 Roma, Italy
[2] Earth and Ocean Science Department, University of British Columbia, 6334 Stores Road, V6T 1Z4 Vancouver BC, Canada

E-mail: dgiordan@uniroma3.it and daniele_giordano@hotmail.com

Received 2 January 2007
Published 25 April 2007
Online at stacks.iop.org/JPhysCM/19/205148

Abstract

Viscosity is the single most important property governing the efficacy, rates, and nature of melt transport. Viscosity is intimately related to the structure and thermodynamics properties of the melts and is a reflection of the mechanisms of single atoms slipping over potential energy barriers. The ability to predict melt viscosity accurately is, therefore, of critical importance for gaining new insights into the structure of silicate melts. Simple composition melts, having a reduced number of components, offer an advantage for understanding the relationships between the chemical composition, structural organization and the rheological properties of a melt. Here we have compiled a large database of ∼970 experimental measurements of melt viscosity for the simple chemical systems MAS, CAS and MCAS. These data are used to create a single chemical model for predicting the non-Arrhenian viscosity as a function of temperature (T) and composition (X) across the entire MCAS system. The T-dependence of viscosity is accounted for by the three parameters in each of the model functions: (i) Vogel–Fulcher–Tamman (VFT); (ii) Adam–Gibbs (AG); and (iii) Avramov (AV). The literature shows that, in these systems, viscosity converges to a common value of the pre-exponential factors (A) that can be assumed to be independent of composition. The other two adjustable parameters in each equation are expanded to capture the effects of composition. The resulting models are continuous across T–X space. The values and implications of the optimal parameters returned for each model are compared and discussed. A similar approach is likely to be applicable to a variety of non-silicate multicomponent glassforming systems.

[3] Author to whom any correspondence should be addressed.

1. Introduction

Early models for predicting the viscosity of silicate melts were developed using viscosity measurements that spanned relatively small ranges of temperature and viscosity. The data, derived from these restricted ranges of experimental conditions, were generally linear in reciprocal temperature and, thus, the early models adopted a strictly Arrhenian formulation [1, 2]. The experimental data available, now, make it very clear that most silicate melts have a non-Arrhenian temperature (T) dependence (e.g. [3]). The literature on the potential connections between the properties and structure of liquids and glasses is vast, reflecting the importance of this issue. Many excellent reviews are available [3–10]. One area where there is substantial room for improvement is in the construction of models that have a capacity to predict the viscosity of silicate melts as a function of melt composition and temperature.

Our purpose is to model the rheological properties of silicate melts in the chemical system MgO–CaO–Al_2O_3–SiO_2 (MCAS). This system contains melts showing *strong* (Arrhenian) to *fragile* (non-Arrhenian) temperature dependence and there is also an extensive database (table A.1 in the appendix) of published viscosity experiments [11–22] (figure 1(A)). The main positive aspect of using these simple chemical systems is the reduced number of components needed to describe their compositional variations. Intuitively, the reduced number of chemical components should make it easier to identify the effects and, perhaps, the speciation or structural role(s) played by each component within the melt [23]. It is because of this possibility that systems such as MAS, CAS, and MCAS have been adopted as reference systems for such a wide range of experimental (for example, calorimetric, dilatometry, viscosimetric, spectroscopic; e.g. [24–27]) and molecular dynamic (e.g. [7–9, 28]) studies.

Our analysis of viscosity in the larger MCAS system is based on experimental measurements on 28, 59 and 19 different melt compositions from MAS, CAS, and MCAS, respectively. The corresponding numbers of published experimental data are 153, 595 and 220, respectively ($\Sigma = 968$). The sources of data are reported in the literature [11–22] and in table A.1 in the appendix. We use these datasets to construct compositional-based non-Arrhenian models for melt viscosity. There are three preferred equations for accommodating the non-Arrhenian T-dependence of silicate melts, including:

(a) Vogel–Fulcher–Tammann (VFT) [29, 30]: $$\log \eta = A_{\mathrm{VFT}} + B_{\mathrm{VFT}}/(T - C_{\mathrm{VFT}}); \quad (1)$$

(b) Adam and Gibbs (AG) [31]: $$\log \eta = A_{\mathrm{AG}} + B_{\mathrm{AG}}/[T \log(T/C_{\mathrm{AG}})]; \quad (2)$$

and

(c) Avramov (AV) [32]: $$\log \eta = A_{\mathrm{AV}} + (B_{\mathrm{AV}}/T)^{C_{\mathrm{AV}}}; \quad (3)$$

where η is the viscosity in Pa s, T is the absolute temperature, and A, B and C are adjustable parameters [29–32]. Equation (2) constitutes an approximation of the original AG expression [31] and assumes ΔCp to be constant and independent of temperature.

Our analysis shows that chemical models based on these three non-Arrhenian equations reproduce the experimental data as a function of composition and temperature equally well. However, the degree and nature of covariation between model parameters (e.g. B and C) for each model are quite different. The corresponding parameters derived for each model (e.g. equations ((1)–(3))) can vary by 200%. The model values of B and C appear to correlate well with simple chemical parameters such as NBO/T [23, 33–35] and SM [33, 35], however these parameters alone cannot capture the behaviour of melt viscosity across the full range of temperature and composition found in this simple system.

2. Theoretical and compositional models

In each of the three non-Arrhenian equations (e.g. (1)–(3)), the parameter A is a pre-exponential term and B represents a pseudo-activation energy related to the potential energy barriers obstructing the structural rearrangement of the liquid. In the VFT and AG expressions, the C parameter represents a lower temperature limit (e.g. Kauzmann temperature) for viscous flow [36, 3, 37–39]. In essence, the C-parameter represents an indication of the dynamical states available for new structural configurations. In contrast, C_{AV} is a measure of melt fragility which is an indication of the non-Arrhenian (versus Arhennian) T-dependence of the melt [3, 32].

Our optimization strategy assumes that the pre-exponential terms (A) for each model (equations ((1)–(3))) are unknown constants. This assumption is consistent with results from previous theoretical [40–42], experimental (e.g. [43, 44]), and numerical studies [22, 45, 46]. Compositional dependence is therefore accommodated solely by variations in B and C terms (see below). In order to be able to compare results from the three different models, we have assumed an identical expression for the compositional dependence of the B and C parameters, given by:

$$B = b_1\mathrm{SiO_2} + b_2\mathrm{Al_2O_3} + b_3\mathrm{MgO} + b_4\mathrm{CaO} + b_{1,3}\mathrm{SiO_2}(\mathrm{MgO} + \mathrm{CaO}) + b_{2,3}\mathrm{Al_2O_3}\ (\mathrm{MgO} + \mathrm{CaO}) \tag{4}$$

and

$$C = c_1\mathrm{SiO_2} + c_2\mathrm{Al_2O_3} + c_3\mathrm{MgO} + c_4\mathrm{CaO} \tag{5}$$

where b_i, b_{ij} and c_i are adjustable parameters. The optimization problems are solved by chi-square minimizations, performed over the all ($N = 968$) experiments (more details on the minimization strategy can be found in previous work on other chemical systems [22, 44, 47]). The 11 coefficients defined in equations (4) and (5) suffice to compute the values of B and C for any melt composition within the systems considered. We adopted the minimum number of quadratic terms in equation (4) necessary to reproduce the original datasets; the inclusion of additional terms did not yield significant improvement in the fittings. The two quadratic terms in equation (4) reflect that the main non-ideal interactions are between the main structure former cations (Si, Al) and the main modifier cations (Ca, Mg). Equation (5) implies that the non-ideal contributions to C are negligible. The calculated values of B and C, when combined with the appropriate model value of A (e.g. equations (1)–(3)) can be used to compute viscosity for a specific melt composition at any temperature.

3. Results

Table 1 reports the optimal values for the constant A (pre-exponential factor) and for the compositional coefficients for the B and C parameters: b_i, b_{ij}, and c_i. We also report the 1σ uncertainties on these adjustable parameters. The recalculated values of B and C for all melt compositions are reported for the three models representing the different non-Arrhenian equations ((1)–(3)) in table A.2 (appendix).

The ability of the VFT, AV and AG models to reproduce the original experimental database is summarized in figure 1. The multicomponent chemical models based on the VFT, AG and AV equations reproduce almost all of the original data to within 0.5 log-units. The root-mean-square errors (RMSE) for each model are essential the same (0.20–0.22; figure 1). The largest deviations between model and observation occur at high values of viscosity ($>10^{10}$ Pa s). The inset diagrams within each plot (figures 1(B)–(D)) show the distribution of residuals relative to

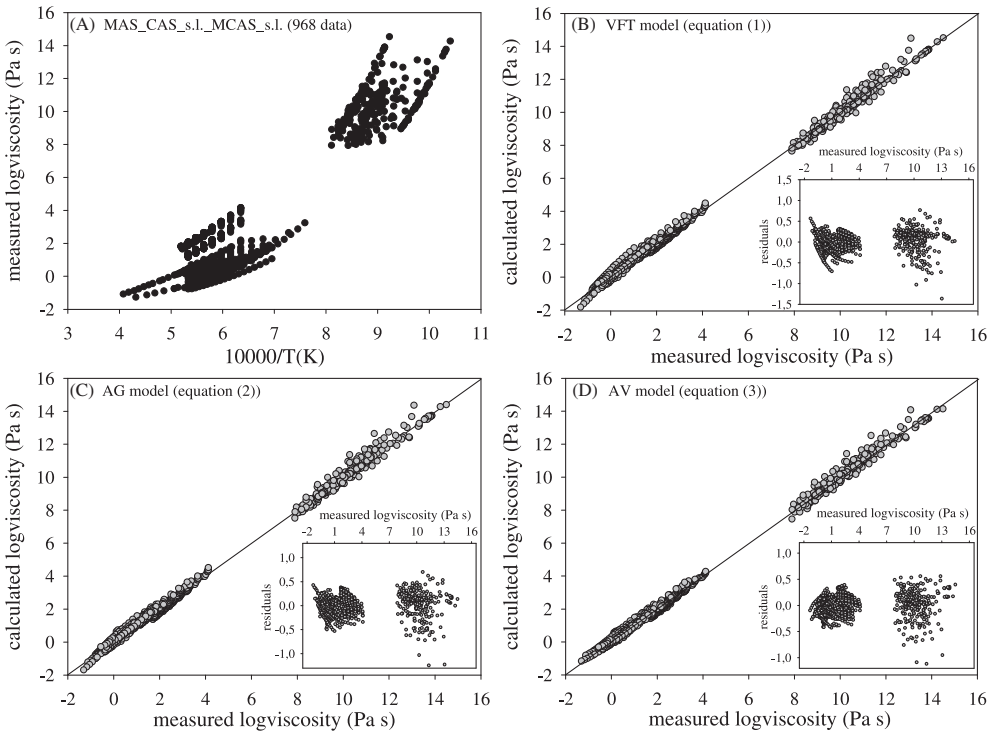

Figure 1. (A) Experimentally measured values ($N = 968$) of melt viscosity versus reciprocal temperature (K) for melt compositions in MCAS system [20–22]. Calculated versus measured $\log \eta$ values for the three models: (B) VFT (equation (1)); (C) AG (equation (2)) and (D) AV (equation (3)). Insets map the model deviations against observed values of $\log \eta$.

the value of melt viscosity; the residuals are evenly distributed and show no systematic patterns. It is clear, therefore, that the three models are equally capable of predicting melt viscosity across the full T–X range found in the MCAS system.

The optimal values of A for each model are: (i) $A_{\mathrm{VFT}} = -4.67(\pm 0.06)$; (ii) $A_{\mathrm{AG}} = -3.68(\pm 0.05)$; and (iii) $A_{\mathrm{AV}} = -1.58(\pm 0.04)$ Pa s (table 2). The value of $A_{\mathrm{VFT}}(-4.67)$ is very similar to values obtained in previous viscosity models for synthetic [43–45] and natural melts [22, 35, 46]. The A_{VFT} value also agrees very well with theoretical [40–42] and numerical [22] estimates on the high-temperature limits to melt viscosity. The value of A_{AG} is approximately $+1$ log units higher than the optimal value for A_{VFT} and this is also in accordance with values found in previous numerical models [22]. This relationship between model values of A_{VFT} and A_{AG} is observed for most melts; optimal values of A_{AG} for the same melt are generally $+1$ units higher than the optimal value of A found using the VFT equation [17, 20–22]. The value of A_{AV} is substantially different (-1.58 ± 0.04) but agrees well with the limiting values established by Avramov [32, 48, 49]. The differences between the model values of A_{AV}, A_{VFT}, and A_{AG} reflect the forms of the fundamental equations (equations (1)–(3)). In the case of the Avramov equation, the difference results from the rate at which the term $[B/T(K)]^C$ approaches the limiting value of 0 compared to the terms $(B/(T - C)$ and $B/(T^* \log(T/C))$. In terms of obtaining an estimate on the high-T limits to silicate melt viscosity (e.g. A), it would appear that the VFT model is the most effective,

Table 1. Results of global optimizations of experimental datasets for compositional coefficients in models based on the VFT, AG and AV equations. Coefficients are defined in equations (4) and (5) and are reported with 1σ uncertainties. Also reported is the RMSE for each model.

		VFT (equation (1))		AG (equation (2))		AV (equation (3))	
Term	Definition	Parameter	±	Parameter	±	Parameter	±
A	Log η_∞	−4.67	0.064	−3.68	0.052	−1.58	0.0425
b_1	SiO_2	107.384	1.329	73.506	1.371	39.146	0.462
b_2	Al_2O_3	58.607	2.899	26.979	2.059	20.344	0.740
b_3	MgO	85.317	3.433	56.782	2.084	29.485	0.405
b_4	CaO	73.746	2.782	43.145	1.462	29.419	0.331
$b_{1,3}$	SiO_2*MC	−1.943	0.053	−1.525	0.030	−0.631	0.012
$b_{2,3}$	Al_2O_3*MC	−1.251	0.077	−0.759	0.045	−0.231	0.013
c_1	SiO_2	6.042	0.101	5.223	0.122	0.0184	0.001
c_2	Al_2O_3	10.190	0.148	9.498	0.174	0.042	0.001
c_3	MgO	7.213	0.147	7.263	0.179	0.061	0.001
c_4	CaO	9.626	0.087	10.307	0.105	0.070	0.001
Std. err.		0.224		0.217		0.200	

MC denotes (MgO + CaO).

followed by the AG formulation. The model value of A_{AV}, the high-T limit to melt viscosity, is $10^{-1.58}$ Pa s, and this is unrealistically high given that many melts (even in this system) have measured viscosities close to [16, 49] or lower than [43, 44] this value.

4. Compositional coefficients

The optimal values for the compositional coefficients listed in table 1 provide insight into the relative contributions of each oxide to both the activation energy (B) and the characteristic C values of the silicate melt. The relative contributions of the oxides to the linear component of the B term are, independently of the model equation used, $SiO_2 > MgO \geqslant CaO > Al_2O_3$. The nonlinear contributions to B can be equal or greater than the linear contribution. Nonlinear contributions to B_{VFT} values range from 20 to 115%. Similarly, the nonlinear component in B_{AG} ranges from 25 to 190% and from 17 to 85% for B_{AV}. The contribution of the nonlinear component to B is greatest in the most depolymerized melts which show the greatest deviation from Arrhenian behaviour (e.g. fragile melts). In contrast, values of C are controlled mainly by CaO and Al_2O_3, where MgO and SiO_2 play subordinate roles.

Lastly, we examine the isothermal variation of viscosity at four different temperatures (900, 1200, 1400 and 1700 °C) for the melts within the MCAS system as a function of SM, NBO/T (figures 2(A), (B), respectively). The computed values of viscosity vary and decrease smoothly with increasing SM at constant temperature (figure 2(A)). The best-fit curves fitted to calculated values of isothermal viscosity predicted by Giordano *et al*'s [35] model for natural silicate melts are also plotted (lines in the figure). At high temperature this model [35] nicely predicts isothermal viscosities as a function of SM, for both natural melts and melts in the MCAS system. However, at temperatures below 1200 °C the model predicts substantially lower values of viscosity for a given value of SM. Similarly to figure 2(A), figure 2(B) shows the calculated values of viscosity as a function of the structural-chemical parameter NBO/T at 900, 1200, 1400, and 1700 °C. The calculated values of viscosity vary smoothly with NBO/T but, relative to the SM-parameter [33, 35], the NBO/T-based trends (solid and dashed lines)

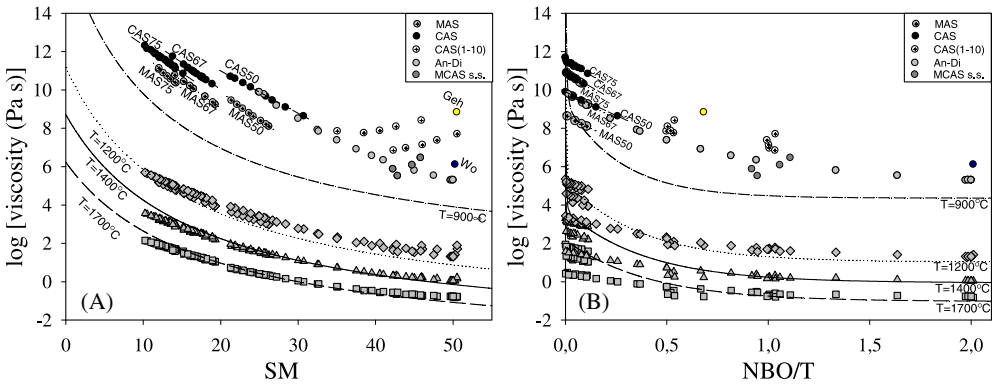

Figure 2. Isothermal viscosity at four temperatures (900 °C, circles; 1200 °C, diamonds; 1400 °C, triangles; and 1700 °C, squares) plotted against melt composition represented by (A) the SM parameter and (B) NBO/T. Values of log η are calculated from the model based on the VFT equation (equation (1); table 1). Lines in (A) are the best-fit isothermal viscosity curves predicted by a published model [35], calibrated for multicomponent natural silicate melts: 1700 °C (dashed); 1400 °C (solid); 1200 °C (dotted); and 900 °C (dash and dot). Lines in (B) are the best-fit isothermal curves predicted, according to a model proposed by [35] and calibrated in respect to the NBO/T parameter [23], similarly to what was done in [33].

do not accurately reproduce melt viscosity in the MCAS system (symbols). In this regard, the SM parameter appears to capture more accurately the isothermal viscosity variations in both natural and synthetic (e.g. MCAS) melt systems. However, neither SM nor NBO/T suffice to describe the compositional controls on melt viscosity (figure 2).

5. Model comparison

We have built three separate compositionally based models (equations (1)–(3)) for predicting non-Arrhenian viscosity in the chemical system MCAS. Although the three equations have substantially different forms, they share some similarities: (i) they have three adjustable parameters (A, B, C) for describing viscosity as a function of temperature; (ii) at high temperature they converge to the value A; and (iii) at low temperatures the functions diverge to infinity. A major difference is that the VFT and AG models converge to infinity as T approaches C, whereas the convergence to infinity is as T approaches 0 for the AV equation.

In figure 3, we compare the three models in terms of the calculated values of B and C for each of the melt compositions in the MCAS system. Values of B derived from the three models show substantial agreement (figures 3(A), (B)). As has already been shown in previous works (e.g. [22, 46]), values of B from the VFT and AG models show the greatest agreement at high values of B where we expect high activation energies and high degrees of melt polymerization. B values from the VFT model tend to be higher than from the AG model. Conversely, the values of B from the AV model are consistently higher than the B_{VFT} values, except at the highest values of B (figure 3(B)). C_{AV} values appear to always be lower than normalized C_{VFT} values (figure 3(D)).

The values of C derived from each of the models show less agreement. The values of C_{VFT} and C_{AG} agree at high values of C, but are systematically different at lower values of C.

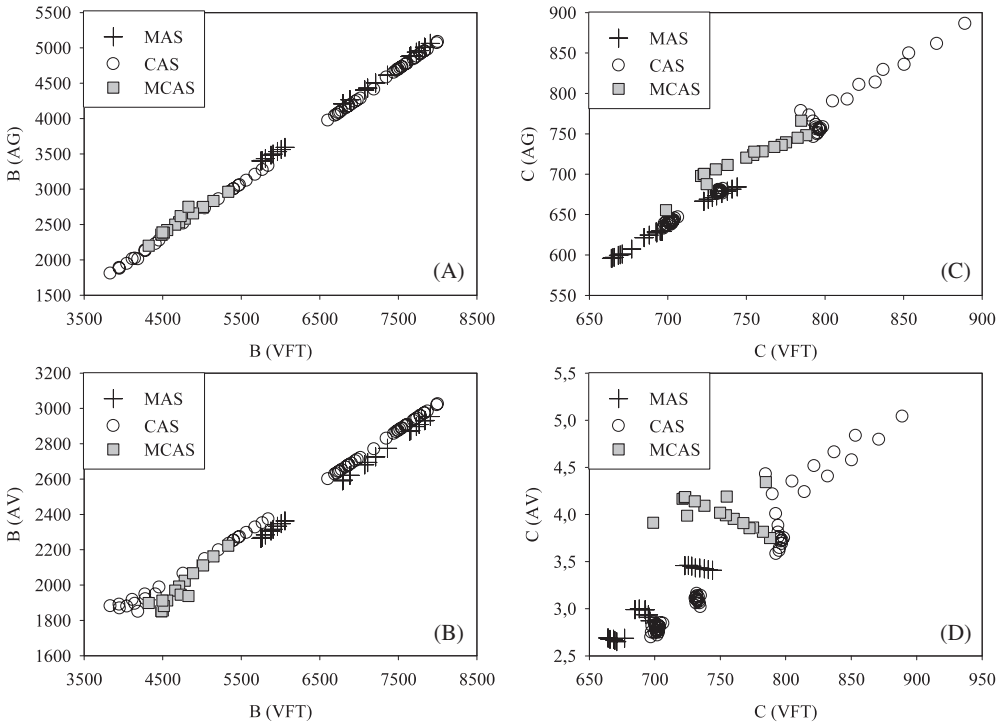

Figure 3. Comparison of values of B and C parameters predicted by the different model equations used for T-dependence of viscosity: (A) B_{AG} versus B_{VFT}; (B) B_{AV} versus B_{VFT}; (C) C_{AG} versus C_{VFT}; and (D) C_{AV} versus C_{VFT}.

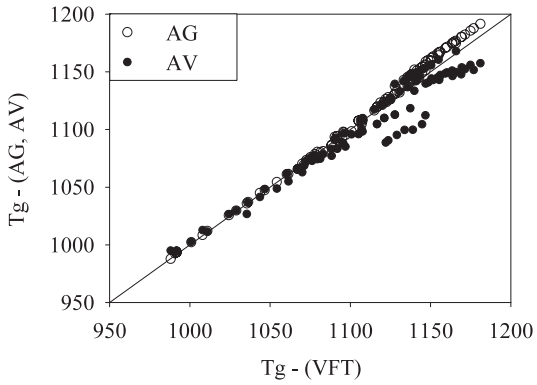

Figure 4. Comparison of computed values of glass transition temperature (T_g). Values of T_g derived from the VFT model are plotted versus the corresponding values of T_g predicted by the AG and AV models.

C_{VFT} values are high relative to values of C_{AG}. For the VFT and AV models, there is no clear relationship between the values of C from each these two models (figures 3(C), (D)).

A direct consequence of these patterns is that, for strong melts, these three models (VFT, AG, AV) recover very similar information on the melt activation energies. This is not true for fragile melts; the implied melt activation energies are substantially different. In the same manner, values of C_{AV} and C_{VFT} show parallel trends for fragile melts (e.g. high values of C) but become increasingly different as melts become stronger. The relationship between values of C_{VFT} and C_{AV} are less coherent and substantially more complicated. On average, values are equivalent for fragile melts but show scatter. As melts become less fragile, there is no relationship between values of C_{VFT} and C_{AV}. As C decreases, C_{VFT} values are higher for a given value of C_{AV}. Such considerations suggest that the VFT model is essentially equivalent to the theoretical Adam Gibbs model [18, 44], whereas the relationship between parameters (e.g. B, C) in the AV model are less easily related to parameters in the VFT and AG models (e.g. equations (1), (2) versus equation (3)).

Another means of exploring the relationships and implications of the three different models is to compare the values of the glass transition temperatures (T_g) for 106 MCAS melt compositions as predicted by each model (figure 4). Here we take T_g to be defined as the temperature at which the melt is expected to have a viscosity of 10^{12} Pa s (e.g. [3, 18, 45, 46]). The calculated T_g deriving from the VFT and AG models (open symbols) have virtually identical values, with average and maximum difference of ∼5 and ∼11 K. The discrepancies between calculated values from the VFT and AV models are substantially larger, with average and maximum deviations of ∼13 and ∼41 K. A comparison of values derived from the AG and AV models shows even larger differences (average ∼17 K and maximum ∼45 K). In both cases, the maximum deviations occur in melts that appear to have high values of T_g. On the basis of this analysis, the VFT and AG models again appear to be equivalent and there is little to no reason to choose one over the other for modelling melt transport properties.

6. Summary

This work shows that compositional-based models are a very powerful tool for predicting both physical and structural properties of silicate melts. Such models are also an aid in exploring the structural roles of each chemical component in the melt. A similar approach is likely to be applicable to a variety of amorphous non-silicate multicomponent systems. Our optimization strategy was used to create three models based on three different equations for the non-Arrhenian T-dependence of silicate melts. Each model assumed that there was a high-temperature limiting value to viscosity (e.g. A); the optimization returned estimates on the value of that adjustable parameter. The relative contributions of the oxides to the linear component of the B term are, independent of the model equation used (e.g. VFT, AG or AV), $SiO_2 > MgO \geqslant CaO > Al_2O_3$. In contrast, values of C are controlled mainly by CaO and Al_2O_3, whereas MgO and SiO_2 play subordinate roles. The results obtained here also show that a multicomponent oxide-based model developed specifically for the MCAS system can substantially improve the prediction of viscosity compared to previous models [19–21]. Within this context, the empirical VFT model appears to represent a fairly good approximation of the theoretical Adam Gibbs model, whereas a more complicated picture emerges from a comparison between VFT and AG models and the more recent, theoretically based Avramov model.

Appendix

Table A.1. List of experimental data available for the systems MAS, CAS, MCAS including: melt composition, number of experiments, and the data source (e.g. 1, 2, 3). (Note: references to data sources: 1 [21]; 2 [20]; 3 [22].)

MAS system			CAS system						MCAS system		
	N	Ref.		*N*	Ref.		*N*	Ref.		*N*	Ref.
MAS75:58	6	1	CAS75a:61	6	1	CAS67b:55	7	1	An_Di	9	3
MAS75:57	3	1	CAS75a:58	7	1	CAS67b:53	7	1	An_Di	13	3
MAS75:55	7	1	CAS75a:56	7	1	CAS67b:52	6	1	An_Di	39	3
MAS75:53	7	1	CAS75a:54	7	1	CAS67b:51	5	1	An_Di	5	3
MAS75:51	7	1	CAS75a:53	7	1	CAS67b:50	6	1	An_Di	5	3
MAS75:49	7	1	CAS75a:50	7	1	CAS67b:49	5	1	An_Di	5	3
MAS75:46	7	1	CAS75a:49	7	1	CAS67b:48	6	1	An_Di	10	3
MAS67b:58a	5	1	CAS75a:47	7	1	CAS50:61	6	1	An_Di	9	3
MAS67b:58b	3	1	CAS75a:45	7	1	CAS50:57	12	1	An_Di	19	3
MAS67:56	5	1	CAS75a:44	7	1	CAS50:54	15	1	An_Di	8	3
MAS67a:53	6	1	CAS75a:41	4	1	CAS50:52	13	1	An_Di	7	3
MAS67b:53	5	1	CAS75b:55	6	1	CAS50:50	10	1	An_Di	19	3
MAS67a:50	5	1	CAS75b:53	6	1	CAS50:48	10	1	An_Di	14	3
MAS67b:50	5	1	CAS75b:52	6	1	CAS50:46	9	1	An_Di	19	3
MAS67a:48	4	1	CAS75b:51	6	1	CAS50:45	8	1	An_Di	6	3
MAS67b:48	4	1	CAS75b:50.5	6	1	CAS50:44	7	1	MCAS15	15	2
MAS67a:46	3	1	CAS75b:50	6	1	CAS1	23	2	MCAS16	10	2
MAS67b:46	3	1	CAS75b:49	6	1	CAS2	29	2	MCAS17	4	2
MAS67:44	3	1	CAS75b:47.5	5	1	CAS3	20	2	MCAS18	4	2
MAS50:55a	4	1	CAS75b:46	5	1	CAS4	18	2			
MAS50:55b	8	1	CAS75b:43.5	5	1	CAS5	11	2			
MAS50:54	5	1	CAS67a:57	7	1	CAS6	15	2			
MAS50:52	9	1	CAS67a:54	7	1	CAS7	17	2			
MAS50:50	8	1	CAS67a:52	7	1	CAS8	18	2			
MAS50:49	7	1	CAS67a:50	7	1	CAS9	10	2			
MAS50:47	6	1	CAS67:50	4	1	CAS10	13	2			
MAS50:45	5	1	CAS67a:47	7	1	Wo	24	2			
MAS50:44	6	1	CAS67a:46	5	1	Geh	10	2			
			CAS67a:41	3	1	An	11	2			
						An	67	2			
Total	153						595			220	

Table A.2. Predicted values of B and C for each experimental melt composition calculated using the three sets of compositional coefficients (table 1) determined for each of the T-dependent equations for viscosity ((1)–(3)).

Label	B_{VFT}	C_{VFT}	B_{AG}	C_{AG}	B_{AV}	C_{AV}	Label	B_{VFT}	C_{VFT}	B_{AG}	C_{AG}	B_{AV}	C_{AV}
CAS75a:61	7349	700	4582	642	2829	2.85	MAS75:58	7644	664	4878	596	2870	2.69
CAS75a:58	7492	698	4694	639	2873	2.82	MAS75:57	7659	665	4888	596	2874	2.69
CAS75a:56	7473	701	4675	641	2866	2.83	MAS75:55	7729	666	4939	597	2897	2.68
CAS75a:54	7444	705	4648	645	2856	2.85	MAS75:53	7765	668	4962	600	2909	2.68
CAS75a:53	7587	701	4762	640	2900	2.80	MAS75:51	7832	670	5011	600	2930	2.66
CAS75a:50	7778	698	4912	635	2958	2.75	MAS75:49	7906	671	5064	601	2954	2.65

Table A.2. (Continued.)

Label	B_{VFT}	C_{VFT}	B_{AG}	C_{AG}	B_{AV}	C_{AV}	Label	B_{VFT}	C_{VFT}	B_{AG}	C_{AG}	B_{AV}	C_{AV}
CAS75a:49	7738	701	4876	639	2944	2.77	MAS75:46	7840	677	5004	607	2931	2.69
CAS75a:47	7831	700	4949	637	2972	2.74	MAS67b:58a	6791	685	4208	622	2591	2.99
CAS75a:45	7838	702	4951	639	2973	2.75	MAS67b:58b	6791	685	4208	622	2591	2.99
CAS75a:44	8004	697	5084	633	3024	2.70	MAS67:56	6800	688	4211	625	2594	3.00
CAS75a:41	7992	702	5067	638	3018	2.72	MAS67a:53	6884	693	4267	628	2621	2.99
CAS75b:55	7522	701	4712	641	2880	2.82	MAS67b:53	6884	693	4267	628	2621	2.99
CAS75b:53	7543	702	4726	642	2886	2.82	MAS67a:50	7070	693	4405	628	2681	2.94
CAS75b:52	7550	703	4730	643	2888	2.82	MAS67b:50	7070	693	4405	628	2681	2.94
CAS75b:51	7503	706	4690	646	2873	2.84	MAS67a:48	7110	695	4431	629	2694	2.94
CAS75b:50.5	7606	703	4773	643	2904	2.81	MAS67b:48	7110	695	4431	629	2694	2.94
CAS75b:50	7615	704	4778	643	2907	2.81	MAS67a:46	7210	696	4504	629	2726	2.91
CAS75b:49	7693	702	4840	641	2930	2.79	MAS67b:46	7210	696	4504	629	2726	2.91
CAS75b:47.5	7715	703	4855	641	2936	2.78	MAS67:44	7361	696	4615	629	2774	2.87
CAS75b:46	7785	703	4909	640	2957	2.77	MAS50:55a	5750	723	3400	666	2264	3.46
CAS75b:43.5	7873	703	4975	640	2983	2.75	MAS50:55b	5750	723	3400	666	2264	3.46
CAS67a:57	6604	732	3972	680	2600	3.16	MAS50:54	5765	726	3407	669	2269	3.46
CAS67a:54	6741	732	4077	678	2640	3.12	MAS50:52	5807	728	3435	671	2284	3.45
CAS67a:52	6718	735	4055	682	2633	3.14	MAS50:50	5878	731	3482	673	2306	3.43
CAS67a:50	6874	733	4175	678	2678	3.09	MAS50:49	5906	734	3499	676	2316	3.43
CAS67:50	6874	733	4175	678	2678	3.09	MAS50:47	5961	738	3533	679	2333	3.42
CAS67a:47	6954	734	4235	678	2701	3.07	MAS50:45	6009	741	3563	682	2348	3.42
CAS67a:46	7021	734	4284	678	2720	3.06	MAS50:44	6058	744	3593	684	2363	3.41
CAS67a:41	7191	735	4411	676	2769	3.02							
CAS67b:55	6694	732	4040	680	2626	3.13	ANDI	4487	723	2360	700	1853	4.19
CAS67b:53	6780	731	4107	677	2652	3.11	ANDI	4502	721	2375	698	1856	4.17
CAS67b:52	6758	734	4087	680	2645	3.12	ANDI	4487	723	2360	700	1853	4.19
CAS67b:51	6830	732	4143	678	2666	3.10	ANDI	4492	723	2364	700	1855	4.18
CAS67b:50	6865	732	4170	677	2676	3.09	ANDI	4487	723	2360	700	1853	4.19
CAS67b:49	6908	733	4201	677	2688	3.08	ANDI	5336	788	2965	748	2224	3.75
CAS67b:48	6981	732	4258	676	2710	3.06	ANDI	4782	760	2585	728	2024	3.96
CAS50:61	5039	794	2729	761	2147	3.88	ANDI	4708	754	2533	724	1992	3.99
CAS50:57	5213	794	2861	758	2197	3.81	ANDI	5146	783	2834	745	2162	3.82
CAS50:54	5346	795	2960	756	2235	3.76	ANDI	5009	775	2742	740	2113	3.86
CAS50:52	5403	796	3001	756	2251	3.74	ANDI	5014	772	2749	736	2112	3.85
CAS50:50	5481	797	3059	755	2272	3.72	ANDI	4888	768	2659	734	2067	3.91
CAS50:48	5568	797	3122	754	2296	3.69	ANDI	4660	750	2498	721	1969	4.02
CAS50:46	5680	795	3206	751	2326	3.64	ANDI	4558	738	2422	712	1913	4.09
CAS50:45	5771	795	3273	749	2351	3.61	ANDI	4515	731	2386	706	1881	4.14
CAS50:44	5846	793	3332	746	2372	3.58	MCAS15	4323	785	2202	766	1899	4.34
CAS1	4411	790	2227	773	1948	4.21	MCAS16	4497	755	2389	728	1912	4.19
CAS2	4282	805	2126	790	1920	4.35	MCAS17	4728	725	2621	688	1946	3.99
CAS3	4147	822	2021	811	1894	4.51	MCAS18	4829	699	2752	656	1938	3.91
CAS4	4046	837	1944	829	1879	4.66							
CAS5	3954	854	1875	850	1869	4.84	Anorthite	5408	799	3002	758	2252	3.75
CAS6	4763	793	2515	765	2064	4.01	AN	5467	797	3047	756	2268	3.72
CAS7	4457	814	2274	792	1987	4.24	Wollastonite	4188	785	2011	778	1849	4.43
CAS8	4277	832	2134	814	1947	4.40	Gehlenite	3836	889	1808	886	1881	5.04
CAS9	4116	851	2012	835	1917	4.58							
CAS10	3948	871	1888	861	1890	4.80							

References

[1] Bottinga Y and Weill D 1972 *Am. J. Sci.* **272** 438–475
[2] Shaw H R 1972 *Am. J. Sci.* **272** 870–93
[3] Angell C A 1991 *J. Non-Cryst. Solids* **131** 13–31
[4] Zallen R 1983 *The Physics of Amorphous Solids* (New York: Wiley–Interscience)
[5] Zarzycki J 1991 *Glasses and the Vitreous State* (Cambridge: Cambridge University Press)
[6] Hansen J P and McDonald I R 1986 *Theory of Simple Liquids* (New York: Academic)
[7] Binder K 1995 *Monte Carlo and Molecular Dynamics Simulations in Polymer Science* (Oxford: Oxford University Press)
[8] Kob W 1995 *Annu. Rev. Comput. Phys.* **3** 1–43
[9] Kob W 1999 *J. Phys.: Condens. Matter* **11** R85–115
[10] Debenedetti P G 1996 *Metastable Liquids: Concepts and Principles* (Princeton, NJ: Princeton University Press)
[11] Kirkpatrick R J 1974 *Am. J. Sci.* **274** 215–42
[12] Cranmer D and Uhlmann D R 1982 *J. Geophys. Res.* **86** 7951–6
[13] Licko T and Danek V 1986 *Phys. Chem. Glasses* **27** 22–6
[14] Neuville D R and Richet P 1991 *Geochim. Cosmochim. Acta* **55** 1011–9
[15] Scarfe C M, Cronin D J, Wenzel J T and Kaufman D A 1983 *Am. Mineral.* **68** 1083–8
[16] Urbain G, Bottinga Y and Richet P 1982 *Geochim. Cosmochim. Acta* **46** 1061–71
[17] Sipp A, Bottinga Y and Richet P 2001 *J. Non-Cryst. Solids* **288** 166–74
[18] Taniguchi H 1992 *Contrib. Mineral. Petrol.* **109** 295–303
[19] Tauber P and Arndt J 1987 *Chem. Geol.* **62** 71–81
[20] Solvang M, Yue Y Z, Jensen S L and Dingwell D B 2004 *J. Non-Cryst. Solids* **336** 179–88
[21] Toplis M J and Dingwell D B 2004 *Geochim. Cosmochim. Acta* **68** 5169–88
[22] Russell J K and Giordano D 2005 *Geochim. Cosmochim. Acta* **69** 5333–49
[23] Mysen B O 1988 *Structure and Properties of Silicate Melts* (Amsterdam: Elsevier) p 354
[24] Richet P, Robie R A and Hemingway B S 1986 *Geochim. Cosmochim. Acta* **50** 1521–33
[25] Webb S and Knoche R 1996 *Chem. Geol.* **128** 165–83
[26] Knoche R, Dingwell D B and Webb S 1992 *Geochim. Cosmochim. Acta* **56** 689–99
[27] Neuville D, Cormier L and Henderson G S 2005 *Massiot Geophysical Research Abstracts* vol 7, p 03160 SRef-ID: 1607-7962/gra/EGU05-A-03160 European Geosciences Union 2005
[28] Morgan N A and Spera F J 2001 *Geochim. Cosmochim. Acta* **65** 4019–41
[29] Vogel D H 1921 Temperaturabhängigkeitsgesetz der Viskosität von Flüssigkeiten *Phys. Z.* **22** 645–6
[30] Fulcher G S 1925 *J. Am. Ceram. Soc.* **8** 339–55
[31] Adam G and Gibbs J H 1965 *J. Chem. Phys.* **43** 139–46
[32] Avramov I 1998 *J. Non-Cryst. Solids* **238** 6–10
[33] Giordano D and Dingwell D B 2003 *Earth Planet. Sci. Lett.* **208** 337–49
[34] Giordano D and Dingwell D B 2003 *J. Phys.: Condens. Matter* **15** S945–54
[35] Giordano D, Mangicapra A, Potuzak M, Russell J K, Romano C, Dingwell D B and Di Muro A 2006 *Chem. Geol.* **229** 42–56
[36] Kauzmann W 1948 *Chem. Rev.* **43** 219–56
[37] Angell C A and Tucker J C 1974 *J. Phys. Chem.* **78** 278–81
[38] Dixon P K 1990 *Phys. Rev.* B **42** 8179–86
[39] Hodge I M and O'Reilly J M 1999 *J. Phys. Chem.* **103** 4171–6
[40] Glastone S, Laidler K J and Eyring H 1941 *The Theory of Rate Processes* (New York: McGraw-Hill) p 486
[41] Myuller R L 1955 *Zh. Prikl. Khim.* **28** 1077–87
[42] Frenkel Y I 1959 *The Kinetic Theory of Liquids. Selected Works* vol 3 (Moscow-Leningrad: Izd. Akad. Nauk SSSR) (in Russian)
[43] Angell C A 1995 *Science* **267** 1924–35
[44] Angell C A, NGai K L, McKenna G B, McMillan P F and Martin S W 2000 *J. Appl. Phys.* **88** 3113–57
[45] Russell J K, Giordano D and Dingwell D B 2003 *Am. Mineral.* **88** 1390–4
[46] Giordano D, Russell J K and Dingwell D B 2006 submitted
[47] Russell J K, Giordano D, Dingwell D B and Hess K U 2002 *Eur. J. Miner.* **14** 417–28
[48] Avramov I, Keding R and Rüssel C 2000 *J. Non-Cryst. Solids* **272** 147–53
[49] Avramov I, Keding R and Rüssel C 2003 *J. Non-Cryst. Solids* **324** 29–35